論　文

Cirrus cloud radiative forcing caused by the 1987 *El Niño* using the nighttime global distribution of microphysical parameters derived from AVHRR

Shuichiro KATAGIRI*, Miho SEKIGUCHI, Teruyuki NAKAJIMA*** and Tadahiro HAYASAKA***

Abstract

We calculated the global cloud radiative forcing (CRF) distributions at the top of the atmosphere (TOA) using the cirrus cloud microphysical parameters of effective radius and optical thickness and the cloud-top temperature (CTT) derived using AVHRR data. The results indicate that cirrus clouds warm the atmosphere, and in particular produce a large warming effect in the tropics. However, radiative forcing of the entire cloud system at the TOA can be negative due to the significant cooling effect of deep convective clouds and optically thick clouds lying at high altitudes.

We computed the dependence of radiative forcing on the effective radius of cloud particles, the optical thickness of the cloud, and the cloud-top temperature and determined that cooling effects occur with clouds when their optical thickness is greater than 4.0~4.5 with a cloud top temperature of 220 K and 2.5~3.0 with a cloud top temperature of 235 K. We also studied cloud radiative forcing in April 1987 (*El Niño* year) and April 1990 (neutral year) and observed that a larger amount of cirrus clouds formed in the tropics off Peru in 1987 than in 1990. However, the globally averaged net cloud radiative forcing was smaller in 1987 than in 1990. Consequently, the temperature distribution of the oceans has a global effect on atmospheric warming and cooling.

Key words: cirrus, cloud radiative forcing, remote sensing

1. Introduction

Clouds have a significant impact on the climate of the earth through modifications of the radiation budget of both incoming solar radiation and outgoing infrared radiation. Clouds partly reflect incoming solar radiation and therefore cool the atmosphere, while they also partly interrupt the infrared radiation emitted from the earth and thereby warm the atmosphere. Accordingly, this radiative impact has been studied intensively. It is believed that the climatic effect of clouds depends on their optical thickness, cloud particle size, and height; low-level and mid-level clouds have a net cooling effect, whereas upper-level clouds mostly have a net warming effect (IPCC 1996; IPCC 2001; IPCC 2007).

The net radiative effect of clouds, combined for all levels, is considered to cool the earth by approximately 20 Wm^{-2} as a global annual mean (Hartmann 1993), although Harrison *et al*. (1990) established that this global mean net cloud radiative forcing shows substantial interannual variation. Ramaswamy and Chen (1997) confirmed that the fluctuation of shortwave cloud radiative forcing tends to be negative in low latitudes throughout the year and during the summer in high latitudes. The potential role of the earth's radiative budget in generating climate feedbacks has been studied by using general circulation models

Received 4 July 2012　　Accepted 12 November 2012

*Center for Atmospheric and Oceanic Studies, Graduate School of Science, Tohoku University, Sendai, Japan
Aoba, Aramakiaza, Aoba-ku, Sendai Miyagi 980-8578, Japan
katagiri@m.tohoku.ac.jp
**Tokyo University of Marine Science and Technology, Tokyo, Japan
***Atmosphere and Ocean Research Institute, The University of Tokyo, Kashiwa, Japan

(GCMs), but it has been difficult to assess the overall effects of clouds on global climate owing to complexities in their feedback processes and radiative properties (Randall *et al*., 1989; Potter and Cess 2004, Ichikawa *et al*., 2012). Therefore, various approaches, such as the variety of parameterizations of cloud processes in various GCMs, have produced large differences in the climate sensitivity values of clouds (Cess *et al*., 1990; IPCC 1996; IPCC 2001; IPCC 2007; Andrews *et al*., 2010; Andrews *et al*., 2012).

The radiative effect of cirrus clouds is particularly ambiguous in these studies. Cirrus clouds are recognized to permanently cover more than 20% of the earth (Liou 1986; Hartmann *et al*., 1992; Liao *et al*., 1995a; 1995b), and together with other high-level clouds, they cover about 30% of the globe at any given time (Wylie and Menzel, 1999; Wylie *et al*., 2005; Stubenrauch *et al*., 2006, 2010; Chepfer *et al*., 2010). Sun *et al*. (2011) used the A-train satellites to observe sub-visual cirrus clouds whose optical thickness was less than 0.3, and found them in 50% of global observations. Cirrus clouds exist at very high altitudes and are composed of ice particles that are almost transparent to solar radiation, although some portion of the infrared radiation from the earth is absorbed, depending on their microphysical properties. Therefore, they are believed to have a warming effect on the climate of the earth (IPCC 1996; IPCC 2001; IPCC 2007). However, it has not yet been determined how much warming or cooling is caused by their radiative effects because their microphysical properties (i.e., cloud optical thickness, ice-particle size, shape, etc.) and physical conditions (i.e., cloud temperature, geometrical structure, etc.) still remain uncertain. Stephens (2005) indicated that the radiative effect of cirrus clouds also varied with surface and lower atmospheric conditions as well as with the clouds' macrophysical and microphysical properties.

Cirrus clouds have therefore become one of the most important research topics in our understanding of the earth's radiative budget and climate system (Charlock and Ramanathan 1985; Baker 1997; Ramanathan 1987; Hansen *et al*., 1998; Ramanathan *et al*., 1989). In this context, many studies and observations of cloud microphysical properties have been undertaken. Several major field projects performed within the International Satellite Cloud Climatology Project (ISCCP) (Schiffer and Rossow 1985; Rossow and Schiffer 1991; Rossow *et al*., 1996) such as the FIRE IFO measurements (Smith *et al*., 1990; Minnis *et al*., 1990; Ackerman *et al*., 1990; Spinhirne *et al*., 1990; Heymsfield *et al*., 1990; Wielicki *et al*., 1990), the FIRE-II IFO measurements (Matrosov *et al*., 1995; Ou *et al*., 1995; Collard *et al*., 1995; Smith *et al*., 1995; Ackerman *et al*., 1995), and other field campaigns have also been conducted (Korolev *et al*., 2001; Boudala *et al*., 2002; McFarquhar *et al*., 2003; Garrett *et al*., 2003).

From around 2000, global cloud microphysical properties derived from satellite data have become available, particularly for low-level clouds (Han *et al*., 1994; Kawamoto *et al*., 2001; Han *et al*., 2002). Doelling *et al*., (2000) have derived cloud radiative forcing at the top of the atmosphere (TOA) from the Advanced Very High Resolution Radiometer (AVHRR) on board the NOAA-12 and NOAA-14 (National Oceanic and Atmospheric Administration) satellites taken over the Arctic Ocean. More recently, the launch of the Moderate Resolution Imaging Spectroradiometer (MODIS) on board the Aqua and Terra satellites has made it possible to determine many cloud parameters. Despite these satellite-borne observations, there is still a scarcity of information, particularly for cirrus cloud distribution and their properties, with regard to any potential impact on global cloud radiative forcing. The microphysical properties of high-level clouds are not included in the MODIS cloud data products.

Studies of high-level clouds are divided into two kinds of research programs depending on the cloud type. The first type is designed to allow an understanding of optically thick high-level clouds associated with the global water circulation system, and the second type studies the optically thin high-level clouds related to the climatic radiation budget. To assess the radiative impact of high-level clouds more precisely, we need to consider these two types of high-level clouds separately. One objective of such a detailed analysis of the effect of high altitude clouds on the global radiation budget is to re-examine the proposal by Ramanathan and Collins (1991) that cirrus clouds work as the thermostat of the earth based on the sea surface temperature.

To assess the radiation budget of cirrus clouds, we used data products derived from the satellite data of Katagiri and Nakajima (2004). These data gave the nighttime global distributions of microphysical properties of cirrus clouds (cirrus cloud particle effective radius, optical thickness, and cloud top temperature) for approximately 9 years between 1986 and 1994 using a three-channel method, which used two infrared window channels (centered on

10.8 μm and 12.0 μm) and a near-infrared channel (3.7 μm) of the AVHRR on board the NOAA-9 and NOAA-11 satellites.

2. Model Description

2.1 Cloud Radiative Forcing

Cloud radiative forcing is defined as the change in net flux at some level in the atmosphere, calculated in response to a perturbation in clouds for otherwise fixed atmospheric parameters (Charlock and Ramanathan 1985). A positive net flux change represents an energy gain and hence net heating of the Earth's system below the level considered, whereas a negative change means an energy loss and net cooling. The definitions of flux are

$$F_\lambda = \int_0^{2\pi}\int_{-\pi/2}^{\pi/2} I_\lambda(\theta, \phi)\cos\theta \sin\theta d\theta d\phi \qquad (1)$$

and

$$F = \int_0^\infty F_\lambda d\lambda \ , \qquad (2)$$

where λ, I_λ, θ, and ϕ denote the wavelength, radiance at λ, zenith angle, and azimuth angle, respectively, at each layer. In this study we considered the flux at the top of the atmosphere. The net cloud radiative forcing of incoming solar radiation, ΔF_S, and outgoing terrestrial radiation, ΔF_L, are defined respectively as

$$\Delta F_S = F_S^{\downarrow} - F_S^{\uparrow} \qquad (3)$$

and

$$\Delta F_L = F_L^{\downarrow} - F_L^{\uparrow}, \qquad (4)$$

where $F_S^{\downarrow}$, $F_S^{\uparrow}$, $F_L^{\downarrow}$, and $F_L^{\uparrow}$ are the downwelling shortwave flux, the upwelling short wave flux, the downwelling longwave flux, and the upwelling longwave flux, respectively. Then, we obtaine the net radiative flux, ΔF_{net},

$$\Delta F_{net} = \Delta F_s - \Delta F_L \ . \qquad (5)$$

Eventually the radiative effect caused by the existence of clouds, named as CRF, is expressed as

$$\Delta F_{cloud} = \Delta F_{net}^{cloudy} - \Delta F_{net}^{clear}, \qquad (6)$$

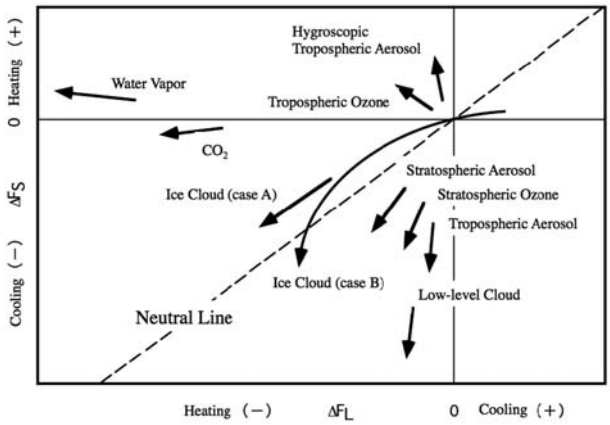

Fig. 1 Outline illustration of shortwave radiative forcings and longwave radiative forcings for several materials. Each arrow indicates the direction when the amount of each material would increase. In case of ice clouds, there could be two directional increases according to what kind of change would happen (case A and case B).

where ΔF_{net}^{cloudy} and ΔF_{net}^{clear} are the net radiative flux with clouds and without clouds, respectively. It is of use to describe the radiative effect caused by existence of clouds as cloud radiative forcing (CRF) defined above. The positive CRF value indicates that the existence of clouds warm the atmosphere, while negative value signifies that clouds have more cooling effect than warming effect. Fig. 1 illustrates that an outline example such that the relationships between shortwave radiative forcing and longwave radiative forcing for several materials. Each arrow indicates the direction when the amount of each material would increase. In case of ice clouds, there could be two directional increases according to what kind of change would happen (case A and case B). An increase of cirrus cloud amount is shown as the case A, and the increase of cirrus clouds optical thickness is shown as the case B. These behaviors imply that the climate change of the earth would be recognized by estimation of the radiative forcing of clouds and/or other materials, for the first step.

2.2. Radiative Transfer Model

We used the radiative transfer code, MSTRAN (Sekiguchi and Nakajima, 2008), for calculating the global radiative flux. The MSTRAN code adopted a *k*-distribution method with two-streams (Nakajima *et al*., 2000) and an 18-band channel subdivided into 6 sub-channels with a wavelength range from 0.2 μm to 200 μm. We calculated the radiative forcing of cirrus clouds at a vertical spatial resolution of

0.5°×0.5° longitude-latitude grids and using the global distribution of the effective cloud droplet radius (*Re*). Cloud droplets were treated as spherical particles, and the optical thickness (τ) was obtained by nighttime AVHRR data analysis (Katagiri and Nakajima, 2004). The effect of non-sphericity produces more scattering effects in a shortwave region, therefore the spherical assumption in this study yields small warming bias in the CRF. The effective radius is defined as

$$R_e = \int_0^\infty r^3 n(r)dr \Big/ \int_0^\infty r^2 n(r)dr. \qquad (7)$$

In our calculation, we assumed that cirrus clouds exist as a single layer under overcast conditions, and the geometrical thickness of cirrus clouds is 2 km. Fig. 2 shows the estimated CRF dependencies on a geometrical thickness of cirrus clouds at TOA and BOA. Fig. 2 indicates our assumed geometrical thickness causes underestimation of the CRF at TOA when actual clouds layer is geometrically thinner than the assumption, while cause overestimation when thicker, on the other hands, at BOA we overestimate when thinner and underestimate when thicker.

We used a log-normal distribution for the particle-size distribution *n(r)*. The temperature profiles, the water vapor profiles, and SST distribution were obtained from the ECMWF (European Centre of Medium-Range Weather Forecasts) reanalysis data set (ECMWF 1995) for each grid. The other gaseous profiles were assumed to be as used in the US standard atmosphere model composed by the Air Force Geophysics Laboratory (AFGL). As yet, there is no published solution of the phase function of non-spherical ice particles for the infrared region; therefore, we assumed the cirrus cloud particle shape to be spherical. In reality, these particles exist in a variety of shapes (Yoshida *et al*., 2010); therefore, we assumed that this non-sphericity would result in greater sideways scattering. This scattering effect by small ice particles in the infrared region is, however, negligible, and the dominant effect is for emissivity; hence, our assumptions are sufficient for an estimation of Cloud Radiative Forcing (CRF).

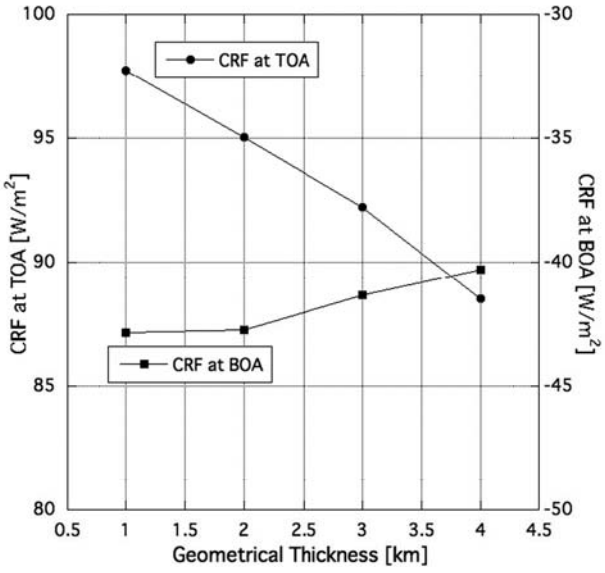

Fig. 2 CRF dependencies on a geometrical thickness of cirrus clouds at TOA and BOA. Calculated with a cloud top height of 10 km and an optical thickness of 1.5.

3. Results and Discussion

3.1. *El Niño* and Cirrus Cloud Radiative Forcing

Ramanathan and Collins (1991) proposed a thermostat effect of cirrus clouds such that as the sea surface temperature (SST) increases in the tropics, there is a corresponding increase in cirrus clouds with high reflectance, which then reduce the surface temperature and stabilize the atmosphere to further suppress formation of cirrus clouds, ensuring negative feedback between SST and the amount of cirrus cloud. To examine this hypothesis using our data sets as shown in Fig. 6, we calculated the CRF for the month of April in an *El Niño* year (1987) and the same month in a neutral year (1990). These two years had a multivariate ENSO index of approximately 2 and 0.2 (Wolter and Timlin 2011), respectively. Although *El Niño* had also occurred in 1991 and 1992, we used data for 1987 because we found the volcanic ashes world-widely spread and affected on the signal from high-level clouds aftermath of Mt. Pinatubo's eruption (Katagiri and Nakajima 2004).

Fig. 3 shows the calculated monthly mean global net CRF distributions for April 1987 (upper panel) and April 1990 (lower panel). We note that our analysis carried out in Katagiri and Nakajima (2004) took two-layer clouds into account. Our definition of cirrus clouds with τ (range between about 0.5 and 3.0) and cloud-top temperature (CTT; <250 K; ≈470 hPa) almost corresponds to the ISCCP definition of cirrus clouds such as the height above 440 hPa and the optical thickness below 3.6 (Katagiri and Nakajima, 2004). The amount of cloud in our gridded box is defined as the frequency of occurrence in one month. The regional values are presented in Fig. 3, and other related information is summarized in Table 1, where averages are calculated with the amount of cloud taken

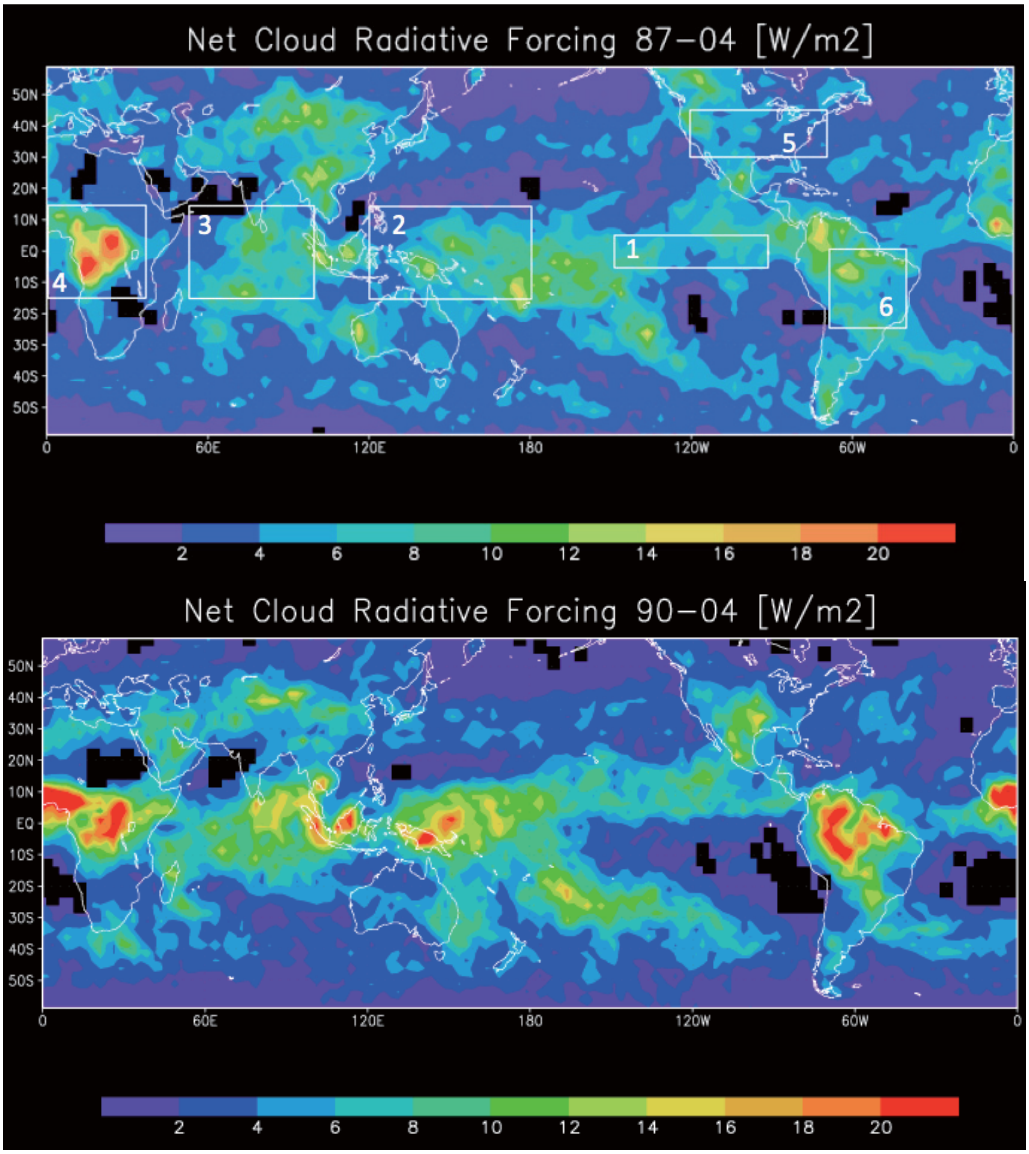

Fig. 3 Global distribution of calculated monthly mean net CRF for April 1987 (upper panel) and for April 1990 (lower panel), respectively.

Table 1 Regional differences in CTT, amount of cirrus cloud, and net CRF between April 1987 and April 1990. Numbers in the first column indicate the gridded box in Fig. 3.

Alea	Longitude	Latitude	CTT [deg]	Cloud Amount	SST [degC]	Net CRF [Wm^{-2}]
1: Off Peru	90°W–150°W	5°N–5°S	−4.16	0.033	0.387	2.06
2: West Pacific Ocean	120°E–180°E	15°N–15°S	1.71	−0.045	−0.296	−2.93
3: Indian Ocean	50°E–100°E	15°N–15°S	1.51	−0.035	0.156	−2.71
4: Central Africa	0°E–40°E	15°N–15°S	3.3	−0.035	—	−2.97
5: North America	70°W–120°W	30°N–45°S	−0.98	−0.028	—	−1.46
6: South America	40°W–70°W	0°N–25°S	1.45	−0.048	—	−3.59
Global	180°E–180°W	60°N–60°S	−0.73	−0.0088	—	−0.05

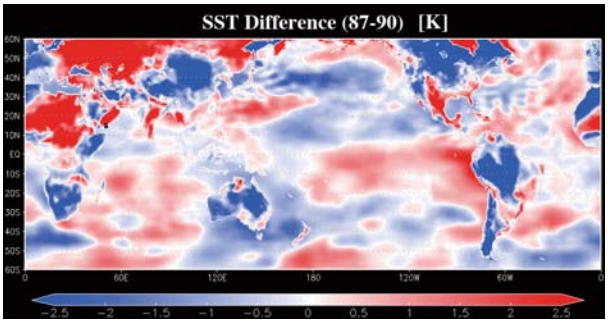

Fig. 4　Sea surface temperature difference between April of 1987 and 1990.

into account. The amounts of cirrus cloud off the coast of Peru (90˚W to 150˚W; 5˚N to 5˚S) were 0.11 in 1987 and 0.07 in 1990. The SST difference between 1987 and 1990 is shown in Fig. 4 and also summarized in Table 1. This is a feature of *El Niño* which shows the rise of 0.387˚C in SST off Peru (box 1 in Fig. 3), while 0.296˚C declination appear in the western Pacific Ocean (box 2 in Fig. 3). The SST of the center of the West Pacific Ocean (150˚E–180˚E; 5˚S–5˚N) was 302.3 K and the SST of the center of off Peru (90˚W–130˚W; 5˚S–5˚N) was 300.5 K in 1990, whereas the former was 301.7 K and the latter was 301.1 K. The SST of off Peru gained heat from the West Pacific Ocean during *El Niño*, but the SST was lower than that in the West Pacific Ocean. Over the central Pacific Ocean, the amount of cloud in 1987 was smaller than in 1990, whereas in the western Pacific Ocean, more cirrus cloud was present in 1987. The cirrus CTT was approximately 4˚C lower in 1987 than in 1990 off Peru, and it was approximately 5˚C higher over the western Pacific Ocean in 1987 than in 1990. This is shown in Fig. 5 (lower panel) and also the cloud amount difference between 1987 and 1990 is shown Fig. 5 (upper panel). Fig. 3 also indicates that over the western Pacific Ocean, there was a strong warming of +10～22 Wm^{-2} in 1990, whereas in 1987, the value was lower at +6～14 Wm^{-2}. Central Africa, South America, and the Indian Ocean were also affected by a strong warming of +15～20 Wm^{-2}. Garrett *et al*. (2003) calculated the diurnal net CRF of cirrus with three parameters (i.e., cloud-top temperature, effective radius, and an asymmetry factor) obtained by their airborne measurements for an ocean surface temperature of 29˚C at 10˚N at the vernal equinox. Our results are consistent with their net CRF results calculated with combinations of CTT and *Re* of (−75˚C; 5 μm), (−60˚C; 7 μm), and (−80˚C; 11 μm).

Fig. 3 also indicates that the net CRF of cirrus clouds was smaller in the Intertropical Convergence Zone (ITCZ)

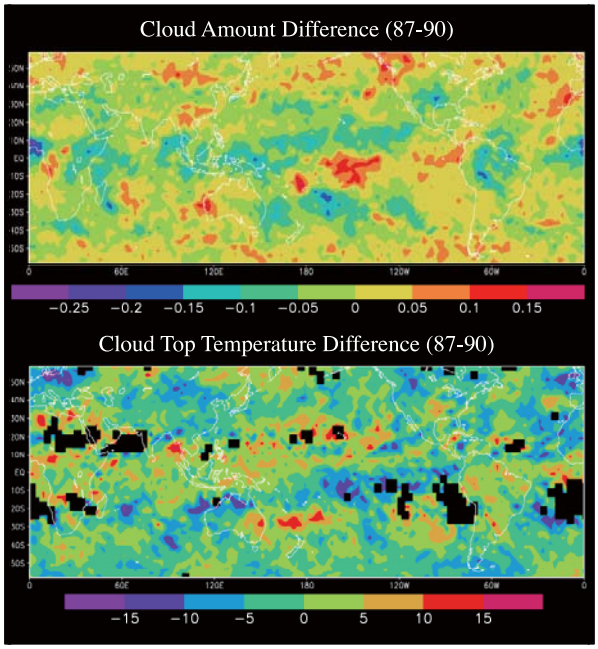

Fig. 5　Cloud amount difference (upper panel) and Cloud top temperature difference (lower panel) between April of 1987 and 1990, respectively.

and South Pacific Convergence Zone (SPCZ) regions in 1987 than in 1990, whereas there were broad regions that tended to have slightly larger CRF values than in 1990. The net CRF off Peru was larger in 1987 than in 1990 by 2 Wm^{-2}, and Central Africa, South America, and the Indian Ocean were warmed by +15～20 Wm^{-2} in 1987 on average, but these strongly heated regions (red～yellow colored area in the lower panel in Fig. 3) lost their area in the upper panel in Fig. 3.

The changes in the distributions of the amount of cirrus cloud, CTT, and CRF summarized in Table 1 suggest that the warming effects over the tropics, attributed to cirrus clouds, decreased because of a large increase in CTT in 1987, although cirrus clouds appeared over larger areas of the tropics in the Pacific Ocean in 1987 than in 1990.

The areal mean net CRF of cirrus clouds in the tropical western Pacific Ocean decreased from +11.01 Wm^{-2} in 1990 to +6.88 Wm^{-2} in 1987. Off Peru, on the other hand, the areal mean net CRF was +3.99 Wm^{-2} in 1990 and +6.04 Wm^{-2} in 1987. Consequently, the net CRF off Peru increased in the *El Niño* year, when the global mean net CRF was +4.98 Wm^{-2} in 1990 and +4.43 Wm^{-2} in 1987. In other words, the global mean net CRF decreased by 0.55 Wm^{-2} due to a reduction in the amount of cirrus clouds reaching high altitudes, which caused large warming effects.

Heymsfield and Miloshevich (2003) reported that the variability of the microphysical properties of cirrus clouds was greater in the lower parts of cirrus clouds than in the upper parts because of the aggregation of falling particles. Okamoto *et al*. (2003) also showed a vertical distribution of cirrus particle sizes, retrieved using a radar-lidar technique, which showed a tendency toward decreasing particle size with altitude; small particles with a radius of 20–30 μm were observed in the upper layer of cirrus clouds. Garrett *et al*. (2003) reported that much smaller effective radii were recorded at low latitudes by airborne measurement using a different approach. We therefore consider that our satellite-retrieved particle-size data shown in Fig. 6 (top panel) for an example, which are more sensitive to small particles within the upper part of the cirrus cloud layer, are more appropriate for evaluating the radiative forcing at the TOA. It is therefore useful to evaluate radiative forcing based on the data sets of Katagiri and Nakajima (2004) shown in Fig. 6 to determine

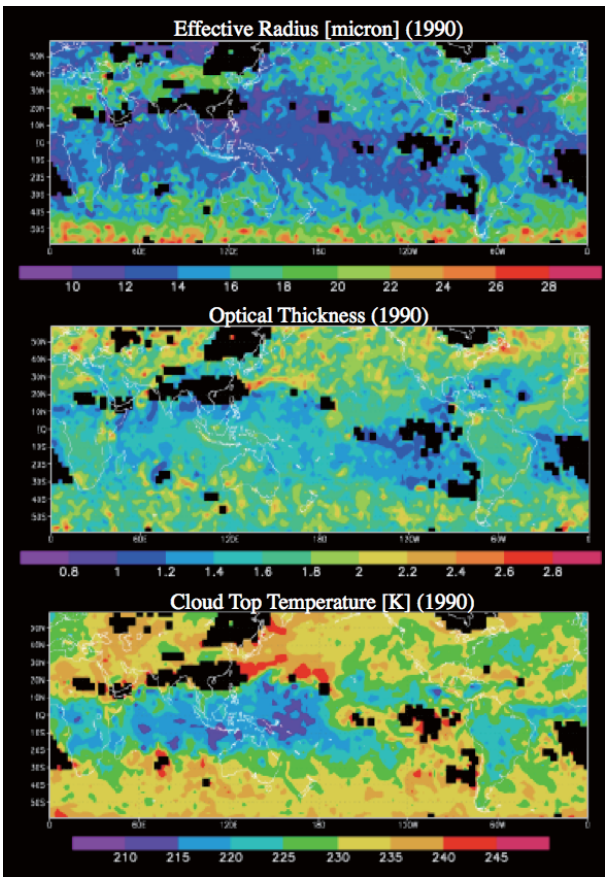

Fig. 6 Used cirrus microphysical data for the CRF estimation, the effective radius distribution (top panel) and the optical thickness distribution (middle panel), and the cloud top temperature (bottom panel), respectively.

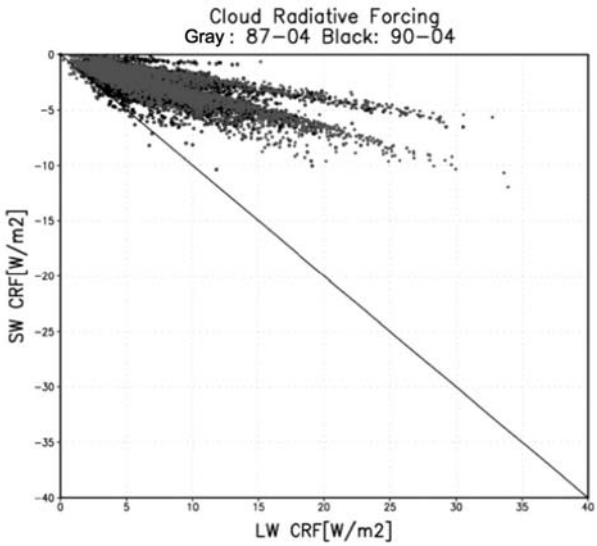

Fig. 7 Scatter plot of the CRF shown in Fig. 3, with gray-colored symbols for April 1987 and black-colored symbols for April 1990, respectively.

the uncertainty in the evaluation of forcing, depending on the cloud microphysical models used in the estimation.

As noted in the previous section, we have assumed overcast conditions, (i.e., a cloud amount of 100%) in each longitudinal and latitudinal pixel of 0.5°. Therefore, cirrus clouds at a high altitude and above a region with high SST have a large potential to change the heat balance of the system by absorbing the longwave radiation emitted from the earth's surface.

Thus, the presence of cirrus clouds has a warming effect on the earth-atmosphere system, particularly when the temperature difference between the earth surface and the cloud top is large. Fig. 7 shows scatter plots of the longwave CRF versus the shortwave CRF values for April 1987 and April 1990 in the tropics (10°N to 10°S), where the gray-colored symbols denote the values for April 1987, and the black-colored symbols denote those for April 1990. This scatter plots indicate that cirrus clouds with high altitude cause strong warming effects at TOA.

Cirrostratus clouds also consist of ice particles and are optically thicker than cirrus clouds lying in high altitudes with the optical thickness of 3.6~23 larger than cirrus clouds' and with the same height (above 440 hPa) as cirrus clouds according to the category of ISCCP. A scatter plot of longwave versus shortwave CRF for clouds with a CTT lower than 250 K in 1990 is shown in Fig. 9, where the dark gray-colored and light gray-colored symbols indicate the tropical cirrus CRF and the mid —and high-latitude cirrus CRF, respectively, and the black symbols denote

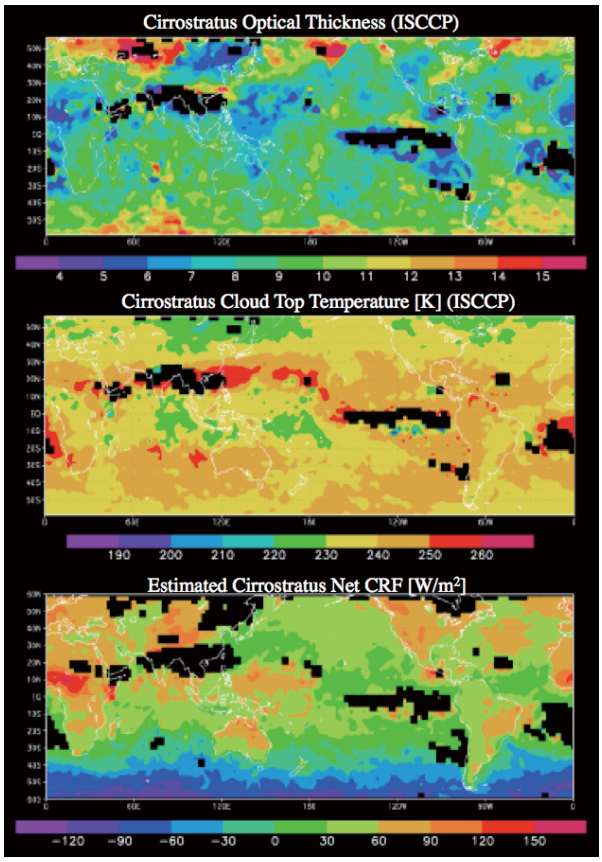

Fig. 8　Used cirrostratus data for the CRF estimation, the optical thickness distribution (top panel) and the cloud top temperature (middle panel) from ISCCP D2, and the estimated CRF of cirrostratus (bottom panel), respectively.

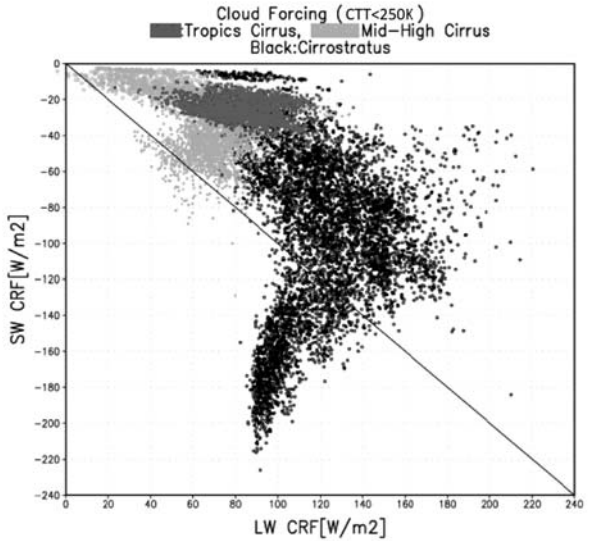

Fig. 9　Scatter plot of CRF caused by ice clouds, such as cirrus and cirrostratus. The black dots denote cirrostratus, the bluish black cirrus clouds in the Tropics, and the light black Mid-High latitude cirrus clouds, respectively.

cirrostratus re-compiled from the ISCCP-D2 cirrostratus clouds data shown in Fig. 8 (top and middle panel) with the effective radius from our results for cirrus clouds shown in Fig. 8 (bottom panel) assuming the global distribution of *Re* for cirrostratus clouds as that of cirrus clouds, because our algorithm cannot retrieve the properties of cirrostratus clouds. The diagonal line in Figs. 7 and 9 represents the neutral condition where the longwave and shortwave CRF are balanced, indicating that cirrus clouds on this line neither cool nor warm the atmospheric system. It is interesting to note in Fig. 7 that the distribution of the scatter plots does not differ for 1987 and 1990 and that cirrus clouds had a similar tendency for shortwave cooling and longwave warming, producing a large warming effect. Fig. 9 shows cirrostratus clouds have larger negative net CRF than cirrus clouds, while there exists a lot of cirrostratus clouds have positive net CRF as same as cirrus clouds. In Figs. 9, a similar tendency to in Fig. 7 can also be noted for the plots to form an arch against the neutral line. This is because the longwave absorptivity increases as a function of τ much more rapidly than the shortwave reflectance does when the cirrus clouds are optically very thin, but the absorptivity approaches an asymptotic value, whereas the shortwave reflectance continues to grow when the cirrus clouds become thick enough, as also explained by the parameterization of Ebert and Curry (1992).

To investigate these properties of CRF, we performed a radiative transfer model calculation of CRF, which is

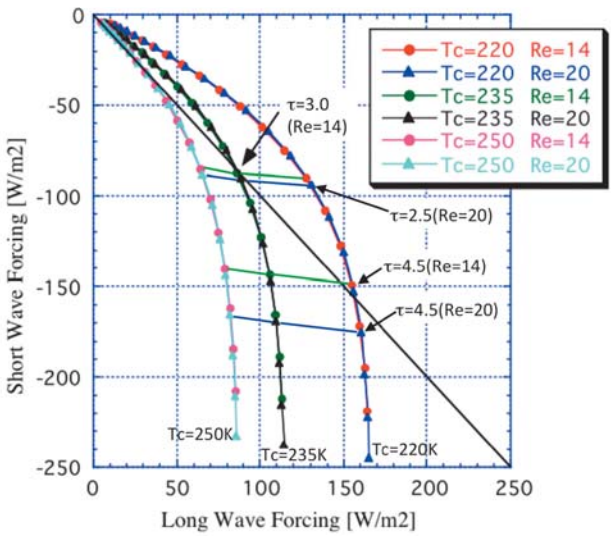

Fig. 10　The relationship between theoretical longwave and shortwave CRF in combination with CTT (220, 235, 250 K) and *Re* (14 and 20 μm), respectively.

presented in Fig. 10 with various CTT values (220, 235 and 250 K), τ (ranging from 0.0 to 6.0), and two *Re* values (14 and 20 μm), where we assumed the AFGL tropical atmospheric profile for the CTT value of 220 K and the mid-latitude summer model for the CTT values of 235 and 250 K. Fig. 10 indicates that for each CTT value, the optical thickness dependence and the particle radius dependence were almost identical in terms of the scatter plot shape, so that curves for different particle radii almost overlap one another. It was also found that a lower CTT produced a larger warming effect when clouds were optically thin, although a higher CTT (such as 250 K) had an almost neutral effect even for optically thin clouds. As the optical thickness increased, the longwave forcing approached an asymptotic value, and the curves for the CTT values of 235 and 220 K straddle the neutral line at τ of 2.5 (*Re*=20 μm), 3.0 (14 μm), and 4.0 (20 μm), and 4.5 (14 μm). Thus, optically thick cirrus clouds have a negative net CRF and cool the system. While some of cirrostratus clouds with optically thinner in its category yield a positive net CRF.

3.2 Thermostat effect of cirrus clouds

Ramanathan and Collins (1991) used the Earth Radiation Budget Experiment (ERBE) data (Barkstrom 1984; Barkstrom and Smith 1986) to assess the effects of cirrus clouds on CRF and presented scatter plots of the shortwave versus the longwave CRF. The statistical analysis indicated a cloud cooling effect on the atmosphere; hence, they concluded that tropical cirrus clouds have a thermostat effect such that the cirrus clouds increase in proportion to the heated SST and subsequently suppress the SST increase. Our computational analysis show that tropical cirrus clouds have a warming effect especially with thin optical thickness, and that cirrostratus clouds have both warming and cooling effect. These effects depend mostly on the temperature difference between the cloud top and the surface summarized in Table 1, and secondly on the optical thickness of high-level clouds. We believe that the difference in the role of cirrus clouds between the analysis by Ramanathan and Collins (1991) and our analysis was caused by difference in the definition of the cirrus clouds. Their scatter plots include all the clouds lying all altitudes, such as cirrus clouds, cirrostratus clouds, deep convection, and stratified clouds in mid-high latitude.

Cess *et al*. (2001) also proposed that anomalous cloud radiative forcing in the tropics during *El Niño* was caused by both the reduced occurrence of high-altitude clouds, ranging from deep convective to thin cirrus, and the increased occurrence of mid-level clouds. They mentioned that the cloud vertical structure was changed by *El Niño* especially for high- and mid-level clouds although small amount of radiative effects due to water clouds were involved in mid-level clouds. Here, our calculated radiative effect of cirrus clouds affected by *El Niño* is a part of the influence of *El Niño* they argued.

Taking account of the frequent existence of mid-level clouds as indicated in ISCCP-D2 data and a decrease in altitude of high-level clouds mentioned by Cess *et al*. in the tropics. (2001), it can be concluded that the cooling agent in the tropics is not high-level clouds but rather mid-level clouds, whereas the high-level clouds generate strong warming effects. According to Harrison *et al*. (1990) an ERBE data analysis indicated that clouds in tropical convective regions reduce the temperature about 100 Wm^{-2} in the SW region. Hence this multi-layered cloud system results in a nearly neutral net CRF, when all clouds are included. Wielicki *et al*. (2002) showed that changes in the radiation budget were caused by changes in mean cloudiness at the tropics. Cloudiness off Peru, from our analysis in Table 1, is consistent with Wielicki *et al*. (2002).

Hence our present study corresponds to the period on the way from the super greenhouse effect to the thermostat effect, and also indicates that the thermostat effect of cirrus clouds introduced by Ramanathan and Collins (1991) is thought to be generated by all clouds over a wide range of altitudes.

4. Conclusion

We made calculations of global CRF distributions using the cirrus cloud microphysical parameters *Re*, τ, and CTT, as derived from AVHRR data (Katagiri and Nakajima 2004). The present study showed that cirrus clouds warm the atmosphere; in particular, in the tropics, cirrus clouds produce a large warming effect because the temperature of cirrus clouds was estimated to be very low in our analysis. Although the overall effect of cirrus clouds was to warm the atmosphere, it was found that low —and mid-level clouds negate this warming effect by bringing a longwave and a shortwave CRF balance, producing a slight cooling zone around the neutral line.

Cooling effects occurred when the optical thicknesses of

a high-level cloud (e.g. cirrus and cirrostratus) was greater than 4.5 ($Re=14\,\mu$m) and 4.0 (20 μm) for a CTT of 220 K and around 3.0 ($Re=14\,\mu$m) and 2.5 (20 μm) for a CTT of 235 K.

Furthermore we compared CRF in April 1987 (*El Niño* year) and April 1990, (neutral year), and we observed that a larger amount of cirrus cloud appeared in the tropics off Peru in 1987 than in 1990. This increased amount of cirrus cloud produced a net CRF of 6.04 Wm^{-2} in 1987, 2.05 Wm^{-2} larger than 1990 value of 3.99 Wm^{-2}. However, the globally averaged net value CRF was 4.43 Wm^{-2} in 1987 and 4.98 Wm^{-2} in 1990. Thus, the net CRF was 0.55 Wm^{-2} smaller in 1987 than in 1990, which is the opposite to the situation in the small area studied around Peru. This is because the net CRF in the western Pacific Ocean was 6.88 Wm^{-2} in 1987, while it was 11.01 Wm^{-2} in 1990. Thus, it was 3.13 Wm^{-2} smaller in 1987 than in 1990, indicating a reduction in the amount of high altitude cirrus clouds in 1987 around the western Pacific Ocean.

Acknowledgments

We are grateful to J. Tucker of NASA GSFC and Ryoichi Imasu of the AORI, University of Tokyo ARGASS (AVHRR GAC dataset for Atmosphere and Surface Studies) project for providing us with the AVHRR GAC data used in this study. The present study was partially supported by a Grant-in-Aid for Scientific Research on Innovative Areas No. 22106004 from MEXT, Japan.

References

Ackerman, S. A., W. L. Smith, J. D. Spinhirne and H. E. Revercomb (1990): The 27–28 October 1986 FIRE IFO Cirrus Case Study: Spectral Properties of Cirrus Clouds in the 8–12 μm Window. Mon. Wea. Rev., **118**, 2377–2388.

Ackerman, S, W. L. Smith, A. D. Collard, X. L. Ma, H. E. Revercomb and R. O. Knuteson (1995): Cirrus Cloud Properties Derived from High Spectral Resolution Infrared Spectrometry during FIRE II. Part II: Aircraft HIS Results. J. Atmos. Sci., **52**, 4246–4263.

Allan, R. P., A. Slingo and M. A. Ringer (2002): Influence of dynamics on the changes in tropical cloud radiative forcing during the 1998 *El Niño*. J. Climate, **15**, 1979-1986.

Andrews, T., J. M. Gregory, P. M. Forster and M. J. Webb (2011): Cloud Adjustment and its Role in CO_2 Radiative Forcing and Climate Sensitivity: A Review. Surv. Geophys., DOI 10.1007/s10712-011-9152-0.

Andrews, T., M. A. Ringer, M. Doutriaux-Boucher, M. J. Webb, and W. J. Collins (2012): Sensitivity of an Earth system climate model to idealized radiative forcing, Geophys. Res. Lett., 39, L10702, doi:10.1029/2012GL051942.

Baker, M. B. (1997): Cloud microphysics and climate. Science, **276**, 1072–1078.

Barkstrom, B. R. (1984): The Earth Radiation Budget Experiment (ERBE). Bull. Amer. Meteor. Soc., **65**, 1170–1185.

Barkstrom, B. R. and G. L. Smith (1986): The earth radiation budget experiment: Science and implementation. Rev. Geophys., **24**, 379–390.

Boudala, F. S., Isaac, G. A., Fu, Q. and Cober, S. G. (2002): Parameterization of effective ice particle size for high-latitude clouds. Int. J. Climatol., 22:1267–1284. doi:10.1002/joc.774.

Cess, R. D., G. L. Potter, J. P. Blanchet, G. J. Boer, A. D. Del Genio, M. Deque, V. Dymnikov, V. Galin, W. L. Gates, S. J. Ghan, A. A. Lacis, H. Le Treut, Z. -X. Li, X. -Z. Liang, B. J. McAvaney, V. P. Meleshko, J. F. B. Mitchell, J. -J. Morcrette, D. A. Randall, L. Rikus, E. Roeckener, J. F. Royer, U. Schlese, D. A. Sheinin, A. Slongo, A. P. Sokolov, K. E. Taylor, W. M. Washington, R. T. Wetherald, I. Yagai and M. -H. Zhang (1990): Intercomparison and interpretation of climate feedback processes in 19 atmospheric general circulation models. J. Geophys. Res., **95**, 16601–16615.

Cess, R. D., M. Zhang, B. A. Wielicki, D. F. Young, X.-L. Zhou and Y. Nikitenko (2001): The influence of the 1998 *El Niño* upon cloud radiative forcing over the Pacific warm pool. J. Climate, **14**, 2129–2137.

Charlock, T. P. and V. Ramanathan (1985): The albedo field and cloud radiative forcing produced by a general circulation model with internally generated cloud optics. J. Atmos. Sci., **42**, 1408–1429.

Chepfer, H., S. Bony, D. Winker, G. Cesana, J. L. Dufresne, P. Minnis, C. J. Stubenrauch and S. Zeng (2010): The GCM- Oriented CALIPSO Cloud Product (CALIPSO-GOCCP), J. Geophys. Res., **115**, D00H16, doi:10.1029/2009JD012251.

Collard, A. D., S. A. Ackerman, W. L. Smith, X. Ma, H. E. Revercomb, R. O. Knuteson and S.-C. Lee (1995):

Cirrus Cloud Properties Derived from High Spectral Resolution Infrared Spectrometry during FIRE II. Part III: Ground-Based HIS Results. J. Atmos. Sci., **52**, 4264–4275.

Doelling, D. R., P. Minnis, D. A. Spangenberg, V. Chakrapani, A. Mahesh, S. K. Pope and F. P. J. Valero (2000): Cloud radiative forcing at the top of the atmosphere during FIRE ACE derived from AVHRR data. J. Geophys. Res., **106**, 15279–15296.

Ebert, E. E. and J. A. Curry (1992): A Parameterization of Ice Cloud Optical Properties for Climate Models, J. Geophys. Res., **97**, 3831–3836.

ECMWF (1995): The Description of the ECMWF/WCRP Level III-A Global Atmospheric Data Archive.

Garrett, T. J., H. Gerber, D. G. Baumgardner, C. H. Twohy and E. M. Weinstock (2003): Small, highly reflective ice crystals in low-latitude cirrus. Geophys. Res. Lett., **30**, 2132, doi:10.1029/2003GL018153.

Han, Q., W. B. Rossow and A. A. Lacis (1994): Near-global survey of effective droplet radii in liquid water clouds using ISCCP data. J. Climate, **7**, 465–497.

Han, Q., W. B. Rossow, J. Zeng and R. Welch (2002): Three different behaviors of liquid water path of water clouds in aerosol-cloud interactions. J. Atmos. Sci., **59**, 726–735.

Hansen, J, M. Sato, A. Lacis, R. Ruedy, I. Tegan and E. Matthews (1998): Climate forcing in the industrial era. Proc. Natl. Acad. Sci., **95**, 12753–12758.

Harrison, E. F., P. Minnis, B. R. Barkstrom, V. Ramanathan, R. D. Cess and G. G. Gibson (1990): Seasonal variation of cloud radiative forcing derived from the earth radiation budget experiment. J. Geophys. Res., **95**, 18687–18703.

Hartmann, D. L., M. E. Ockert-Bell and M. L. Michelsen (1992): The effect of cloud type on Earth's energy balance: Global analysis. J. Climate, **5**, 1281–1304.

Hartmann, D. L. (1993): Radiative effects of clouds on Earth's climate. Aerosol-Cloud-Climate Interactions. Hobbs, P. V., Ed., Academic Press, San Diego, CA, USA, 233 pp.

Heymsfield, A. J., Karen M. Miller and James D. Spinhirne (1990): The 27–28 October 1986 FIRE IFO Cirrus Case Study: Cloud Microstructure. Mon. Wea. Rev., **118**, 2313–2328.

Heymsfield, A. J. and L. Milochevich (2003): Parameterization for the cross-sectional area and extinction of cirrus and stratiform ice cloud particles. J. Atmos. Sci., **60**, 936–956.

Intergovernmental Panel on Climate Change (IPCC), edited by Houghton, J. T. *et al*. (1996): Climate Change 1995: The Science of Climate Change. Cambridge Univ. Press, New York, 572 pp.

Intergovernmental Panel on Climate Change (IPCC) edited by Houghton, J. T. *et al*. (2001): Climate Change 2001: The Scientific Basis. Cambridge Univ. Press, New York, 881 pp.

Intergovernmental Panel on Climate Change (IPCC) edited by S. Solomon *et al*. (2007): Climate Change 2007: The Scientific Basis. Contribution of Working Group I to the Fourth Assessment Report of the Intergovernmental Panel on Climate Change. Cambridge Univ. Press, New York, 1009 pp.

Ichikawa, H, H. Masunaga, Y. Tsushima and H. Kanazawa (2012): Reproducibility by Climate Models of Cloud Radiative Forcing Associated with Tropical Convection. DOI:10.1175/JCLI-D-11-00114.1, J. Climte, **25**, 1247–1262.

Katagiri, S. and T. Nakajima (2004): Radiative characteristics of cirrus clouds as retrieved from AVHRR. J. Meteor. Soc. Japan, **82**, 81–99.

Kawamoto, K., T. Nakajima and T. Y. Nakajima (2001): A global determination of cloud microphysics with AVHRR remote sensing. J. Climate, **14**, 2054–2068.

Korolev, A. V., G. A. Isaac, I. P. Mazin, and H. W. Barker (2001): Microphysical properties of continental clouds from in situ measurements. Q.J.R. Meteorol. Soc., **127**: 2117–2151. doi:10.1002/qj.49712757614

Liao, X., D. Rind and W. B. Rossow (1995a): Comparison between SAGE II and ISCCP high-level clouds, Part I: Global and zonal mean cloud amounts. J. Geophys. Res., **100**, 1121–1135.

Liao, X., D. Rind and W. B. Rossow (1995b): Comparison between SAGE II and ISCCP high-level clouds, Part II: Locating cloud tops. J. Geophys. Res., **100**, 1137–1147.

Liou, K. N. (1986): Influence of cirrus clouds on weather and climate processes: A global perspective. Mon. Wea. Rev., **114**, 1167–1199.

McFarquhar, G. M., P. Yang, A. Macke and A. J. Baran (2002): A New Parameterization of Single Scattering Solar Radiative Properties for Tropical Anvils Using Observed Ice Crystal Size and Shape Distributions. J. Atmos. Sci., **59**, 2458–2478.

Matrosov, S. Y., A. J. Heymsfield, J. M. Intrieri, B. W. Orr

and J. B. Snider (1995): Ground-Based Remote Sensing of Cloud Particle Size during the 26 November 1991 FIRE II Cirrus Case: Comparisons with In Situ Data. J. Atmos. Sci., **52**, 4128–4142.

Minnis, P, D. F. Young, K. Sassen, J. M. Alvarez and C. J. Grund (1990): The 27–28 October 1986 FIRE IFO Cirrus Case Study: Parameter Relationships Derived from Satellite and Lidar Data, Mon. Wea. Rev., **118**, 2402–2425.

Nakajima, T., M. Tsukamoto, Y. Tsushima, A. Numaguti, and T. Kimura (2000): Modeling of the radiative process in an atmospheric general circulation model. Appl. Opt., **39**, 4869–4878.

Okamoto, H., S. Iwasaki, M. Yasui, H. Horie, H. Kuroiwa and H. Kumagai (2003): An algorithm for retrieval of cloud microphysics using 95-GHz cloud radar and lidar. J. Geophys. Res., **108**, 4226, doi:10.1029/2001JD001225.

Ou, S. C., K. N. Liou, Y. Takano, N. X. Rao, Q. Fu, A. J. Heymsfield, L. M. Miloshevich, B. Baum and S. A. Kinne (1995): Remote Sounding of Cirrus Cloud Optical Depths and Ice Crystal Sizes from AVHRR Data: Verification Using FIRE II IFO Measurements. J. Atmos. Sci., **52**, 4143–4158.

Potter, G. L. and R. D. Cess (2004): Testing the impact of clouds on the radiation budgets of 19 atmospheric general circulation models. J. Geophys. Res., **109**, doi:10.1029/2003JD004018.

Ramanathan, V. (1987): The role of Earth radiation budget studies in climate and general circulation research. J. Geophys. Res., **92**, 4075–4095.

Ramanathan, V., R. D. Cess, E. F. Harrison, P. Minnis, B. R. Barkstrom, E. Ahmad and D. Hartmann (1989): Cloud radiative forcing and climate: Results from the Earth Radiation Budget Experiment. Science, **243**, 57–63.

Ramanathan, V. and W. Collins (1991): Thermodynamic regulation of ocean warming by cirrus clouds deduced from observations of the 1987 *El Niño*. Nature, **351**, 27–32.

Ramaswamy, V. and C. T. Chen (1997): Linear additivity of climate response for combined albedo and greenhouse perturbations. Geophys. Res. Lett., **24**, 567–570.

Randall, D. A., Harshvardhan, D. A. Dazlich and T. G. Corsetti (1989): Interaction among radiation, convection, and large-scale dynamics in a general circulation model. J. Atmos. Sci., **46**, 1943–1970.

Rossow, W. B. and R. A. Schiffer (1991): ISCCP cloud data products. Bull. Amer. Meteor. Soc., **72**, 2–20.

Rossow, W. B., A. W. Walker, D. E. Beuschel and M. D. Roiter (1996): International Satellite Cloud Climatology Project (ISCCP) documentation of new cloud datasets. WMO/TD737, World Climate Research Programme (ICSU and WMO), 115 pp.

Schiffer, R. A. and W. B. Rossow (1985): ISCCP global radiance data set: A new resource for climate research. Bull. Amer. Meteor. Soc., **66**, 779–784.

Sekiguchi, M., and T. Nakajima (2008): A k-distribution-based radiation code and its computational optimization for an atmospheric general circulation model, J. Quant. Spectrosc. Radiat. Transfer, doi:10.1016/j.jqsrt.2008.07.13.

Smith, W. L. Jr., P. F. Hein and S. K. Cox (1990): The 27–28 October 1986 FIRE IFO Cirrus Case Study: In Situ Observation of Radiation and Dynamic Properties of a Cirrus Cloud Layer. Mon. Wea. Rev., **118**, 2389–2401.

Smith, W. L. Jr., H. E. Revercomb, R. O. Knuteson, F. A. Best, R. Dedecker, H. B. Howell and H. M. Woolf (1995): Cirrus Cloud Properties Derived from High Spectral Resolution Infrared Spectrometry during FIRE II. Part I: The High Resolution Interferometer Sounder (HIS) Systems. J. Atmos. Sci., **52**, 4238–4245.

Spinhirne, J. D. and W. D. Hart (1990): Cirrus Structure and Radiative Parameters from Airborne Lidar and Spectral Radiometer Observations —The 28 October 1986 FIRE Study. Mon. Wea. Rev., **118**, 2329–2343.

Stephens, G. L. (2005): Cloud feedbacks in the climate system: A critical review, J. Clim., **18**, 237–273, doi:10.1175/JCLI-3243.1.

Stubenrauch, C. J., A. Chédin, G. Rädel, N. A. Scott and S. Serra. (2006): Cloud Properties and Their Seasonal and Diurnal Variability from TOVS Path-B, J. Climate, **19**, 5531–5553.

Stubenrauch, C. J., Cros, S., Guignard, A. and Lamquin, N. (2010): A 6-year global cloud climatology from the Atmospheric InfraRed Sounder AIRS and a statistical analysis in synergy with CALIPSO and CloudSat, Atmos. Chem. Phys., **10**, 7197–7214, doi:10.5194/acp-10-7197-2010.

Sun, W., G. Videen, S. Kato, B. Lin, C. Lukashin and Y. Hu (2011): A study of subvisual clouds and their

radiation effect with a synergy of CERES, MODIS, CALIPSO, and AIRS data, J. Geophys. Res., **116**, D22207, doi:10.1029/2011JD016422.

Wielicki, B. A., J. T. Suttles, A. J. Heymsfield, R. M. Welch, J. D. Spinhirne and M. C. Wu, D. O'C. Starr, L. Parker and R. F. Arduini (1990): The 27–28 October 1986 FIRE IFO Cirrus Case Study: Comparison of Radiative Transfer: Theory with Observations by Satellite and Aircraft. Mon. Wea. Rev., **118**, 2356–2376.

Wielicki, B. A., T. Wong, R. P. Allan, A. Slingo, J. T. Kiehl, B. J. Soden, C. T. Gordon, A. J. Miller, S.-K. Yang, D. A. Randall, F. Robertson, J. Susskind, H. Jacobowitz (2002): Evidence for large decadal variability in the tropical mean radiative energy budget. Science, **295**, 841–844.

Wolter, K. and M. S. Timlin (2011): *El Niño*/Southern Oscillation behaviour since 1871 as diagnosed in an extended multivariate ENSO index (MEI.ext). Int. J. Climatol., **31**, 1074–1087.

Wylie, D. P. and W. P. Menzel (1999): Eight years of high cloud statistics using HIRS. J. Climate, **12**, 170–184.

Wylie, D. P., D. L. Jackson, W. P. Menzel and J. J. Bates (2005): Trends in global cloud cover in two decades of HIRS observations. J. Climate, **18**, 3021–3031.

Yoshida, R., H. Okamoto, Y. Hagihara and H. Ishimoto (2010): Global analysis of cloud phase and ice crystal orientation from Cloud-Aerosol Lidar and Infrared Pathfinder Satellite Observation (CALIPSO) data using attenuated backscattering and depolarization ratio, J. Geophys. Res., **115**, doi:10.1029/2009JD012334.